

Review

Microtubule-Targeting Agents: Strategies To Hijack the Cytoskeleton

Michel O. Steinmetz^{1,2,*} and Andrea E. Prota^{1,*}

Microtubule-targeting agents (MTAs) such as paclitaxel and the vinca alkaloids are among the most important medical weapons available to combat cancer. MTAs interfere with intracellular transport, inhibit eukaryotic cell proliferation, and promote cell death by suppressing microtubule dynamics. Recent advances in the structural analysis of MTAs have enabled the extensive characterization of their interactions with microtubules and their building block tubulin. We review here our current knowledge on the molecular mechanisms used by MTAs to hijack the microtubule cytoskeleton, and discuss dual inhibitors that target both kinases and microtubules. We further formulate some outstanding questions related to MTA structural biology and present possible routes for future investigations of this fascinating class of antimetabolic agents.

Agents Targeting the Microtubule Cytoskeleton

The microtubule **cytoskeleton** (see [Glossary](#)) plays pivotal roles in several biological functions, ranging from intracellular trafficking and positioning of cellular components in interphase, the formation of the mitotic spindle during cell division, to the establishment and maintenance of cell morphology and cell motility (reviewed in [1–3]). Because of being implicated in such key cellular activities, compounds that interfere with microtubule cytoskeleton functions have been developed as cytotoxic agents not only for basic research experiments to demonstrate the dependence of cellular processes on microtubules, but most importantly to combat parasites and cancer (reviewed in [4]). Colchicine was the first compound identified as an MTA and is the most commonly used drug to treat gout. The first MTAs approved more than half a century ago for treating lymphomas and various solid tumors were the vinca alkaloids vinblastine and vincristine. An important breakthrough for MTAs was in the early 1990s when paclitaxel (Taxol[®]) became a first-line drug for the treatment of ovarian, breast, bladder, prostate, and lung cancers [4,5]. However, in addition to massive success in the clinic, the application of MTAs is hampered by toxicity and the development of resistance [6,7]. To overcome these challenges, additional chemotherapeutic MTAs such as epothilone (Ixempra[®]), eribulin (Halaven[®]), auristatin (Adcetris[®]), and maytansine (Kadcyla[®]) have been approved by the FDA in the past 10 years and introduced into the clinic either as classical drugs or as **antibody–drug conjugates** (ADCs).

Several dozen different chemical classes of MTAs are known today. The majority of MTAs are natural products or synthetic derivatives thereof that originate from natural sources such as marine sponges, plants, or bacteria (reviewed in [4]). By perturbing **microtubule dynamics** during **mitosis**, MTAs interfere with **mitotic spindle** formation, arrest cells in mitosis, and in many cases promote **apoptotic** cell death, which is the strategy in chemotherapies to combat cancer. However, they also act on interphase microtubule arrays and affect the intracellular trafficking of important molecules and organelles, which is of particular importance in neurons; MTA might thus be beneficial to treat injuries and diseases of the nervous system (reviewed in

Highlights

Structural biology has allowed the identification and detailed characterization of six distinct ligand-binding sites on tubulin. Two sites are targeted by microtubule-stabilizing agents (MSAs); four sites are targeted by microtubule-destabilizing agents (MDAs).

MSAs stabilize microtubules by strengthening lateral and/or longitudinal tubulin contacts in microtubules. MDAs destabilize microtubules by either inhibiting the formation of native tubulin contacts or by hindering the curved-to-straight conformational change of tubulin accompanying microtubule formation.

Different types of anticancer agents that were initially developed against kinases were found to bind also to tubulin as an off-target.

¹Laboratory of Biomolecular Research, Division of Biology and Chemistry, Paul Scherrer Institut, 5232 Villigen, Switzerland
²University of Basel, Biozentrum, 4056 Basel, Switzerland

*Correspondence: michel.steinmetz@psi.ch (M.O. Steinmetz) and andrea.prota@psi.ch (A.E. Prota).

[8]). Based on their activities on microtubules at high concentrations, MTAs can be broadly grouped into microtubule-stabilizing agents (MSAs) and microtubule-destabilizing agents (MDAs). They achieve their effects by either promoting microtubule assembly in the case of MSAs, or by triggering microtubule disassembly into tubulin dimers and small oligomers in the case of MDAs (Box 1). However, at low and clinically relevant concentrations both MSAs and MDAs primarily suppress microtubule dynamics without significantly affecting the microtubule-polymer mass (reviewed in [4]).

Recent advances in the tubulin structural biology field have made it possible to investigate the molecular mechanisms of action of a wide range of different MTAs at the atomic level (Table 1). Notably, until 2013 three distinct MTA-binding sites on tubulin, referred to as the taxane site, the colchicine site, and the vinca site (Figure 1), had been structurally characterized to high resolution. Since then three additional binding sites have been investigated by **X-ray crystallography** and **cryo-electron microscopy** (cryo-EM) in great detail; they are referred to as the maytansine site, the laulimalide/peloruside site, and the pironetin site (Figure 1). In this article we present our current knowledge on the six known tubulin-binding modes of MTAs and review the molecular mechanisms of action of MTAs on tubulin and microtubules. We then describe dual inhibitors that interact with **kinases** and microtubules, a property that represents a challenge in developing target-specific drugs with improved safety profiles. Finally, we discuss possible routes for the development of next-generation MTAs for future use in the clinic.

Tubulin-Binding Modes and Molecular Mechanisms of Action of MSAs

Taxane-Site Ligands

The first atomic level description of the binding of an MTA to tubulin was paclitaxel, whose structure was solved in 1998 based on electron crystallography data obtained from tubulin–paclitaxel zinc-sheets [9,10]. Almost two decades later, X-ray crystallography and cryo-EM enabled the structural

Box 1. Microtubule Structure and Dynamic Instability

At a macroscopic level, microtubules appear as hollow tubes with a diameter of ~25 nm. They are dynamically polymerized from stable $\alpha\beta$ -tubulin heterodimers that align in a head-to-tail fashion into protofilaments. Both the α - and β -tubulin subunits bind GTP; however, only the nucleotide on β -tubulin is hydrolyzed and exchanged. In cells, microtubules typically comprise 13 protofilaments that are aligned side-by-side in a parallel manner. Because $\alpha\beta$ -tubulin heterodimers assemble head-to-tail, and because protofilaments align in parallel, the microtubule is polar with one end exposing β -tubulin subunits (the fast-growing 'plus end') and the other end exposing α -tubulin subunits (the slow-growing 'minus end') (reviewed in [75]). Tubulin dimers in 13-protofilament microtubules follow a three-start helical pattern (i.e., the helix spans three subunits of a protofilament before it completes one turn) where homotypic interactions between tubulin subunits are established, with one exception: at the microtubule lattice seam, α -tubulin subunits from one protofilament contact β -tubulin subunits of the neighboring protofilament.

In the presence of GTP, tubulin–GTP dimers that assume a 'curved' conformation add to growing microtubule ends (Figure I-1). Based on cryo-EM, growing microtubule ends are thought to maintain an open and slightly bent to straight sheet-like structure. Thus, curved tubulin–GTP dimers undergo a gradual 'curved-to-straight' conformational transition upon incorporation into microtubule lattices (reviewed in [3,76]). Because GTP hydrolysis and phosphate release are delayed with respect to microtubule growth, growing ends maintain a cap of GTP–tubulin/GDP•P_i–tubulin dimers (denoted the 'GTP-cap'), which stabilizes the microtubule. Accordingly, the main microtubule shaft is composed of tubulin–GDP dimers (note that the GTP bound to α -tubulin is non-exchangeable and never hydrolyzes). Upon stochastic loss of the GTP-cap, microtubule ends can undergo rapid depolymerization, a process that is characterized by protofilaments peeling off from the microtubule shaft and dissociating into tubulin–GDP dimers and small curved oligomers (Figure I-2). The change from the growing phase to the shrinkage phase is called a 'catastrophe'; the reverse process is called a 'rescue'. The switching between catastrophes and rescues is referred to as 'dynamic instability', a process that is driven by GTP hydrolysis on β -tubulin and which is fundamental to microtubule function (reviewed in [76]). The tubulin assembly–disassembly cycle is completed by exchanging the GDP nucleotide on β -tubulin with GTP (Figure I-3). Notably, MSAs and MDAs shift the equilibrium towards the microtubule polymer (Figure I-1) or tubulin dimers and small oligomers (Figure I-2), respectively, at high compound concentrations.

Glossary

Apoptosis: a biochemical process leading to cell death.

Allostery: the process by which proteins transmit the effect of binding at one site to another, often distal, site.

Antibody–drug conjugates

(ADCs): complex molecules composed of an antibody linked to a cytotoxic agent, which are used in targeted anticancer therapy.

Cryo-electron microscopy (cryo-EM): transmission EM carried out at cryogenic temperatures. The method allows the structural analysis of vitrified macromolecules at high resolution.

Cytoskeleton: a complex network of interlinked protein filaments that extend throughout the cytoplasm of a cell, from the nucleus to the plasma membrane.

Microtubule dynamics: switching behavior between growth and shrinkage of microtubules.

Microtubule lattice seam: a discontinuity in the helical lattice of some microtubules where an α -tubulin subunit from one protofilament contacts a β -tubulin subunit of the neighboring protofilament.

Minus end: the slow-growing end of a microtubule exposing α -tubulin subunits.

Mitotic spindle: microtubule-based cytoskeletal structure of eukaryotic cells that forms during mitosis to separate and distribute sister chromatids equally between daughter cells.

Mitosis: the phase of the cell cycle when replicated chromosomes are distributed between daughter cells.

Kinases: enzymes that catalyze the transfer of phosphate groups from ATP to a specific substrate.

Plus end: the fast-growing end of a microtubule exposing β -tubulin subunits.

Synchrotron: an extremely powerful source of X-rays that are produced by high-energy electrons as they move along a circular path.

X-ray crystallography: method to determine the atomic structure of macromolecules in a crystal. The atoms in the crystal cause a beam of incident X-rays to diffract in many specific directions, and this can be exploited to produce a 3D picture of

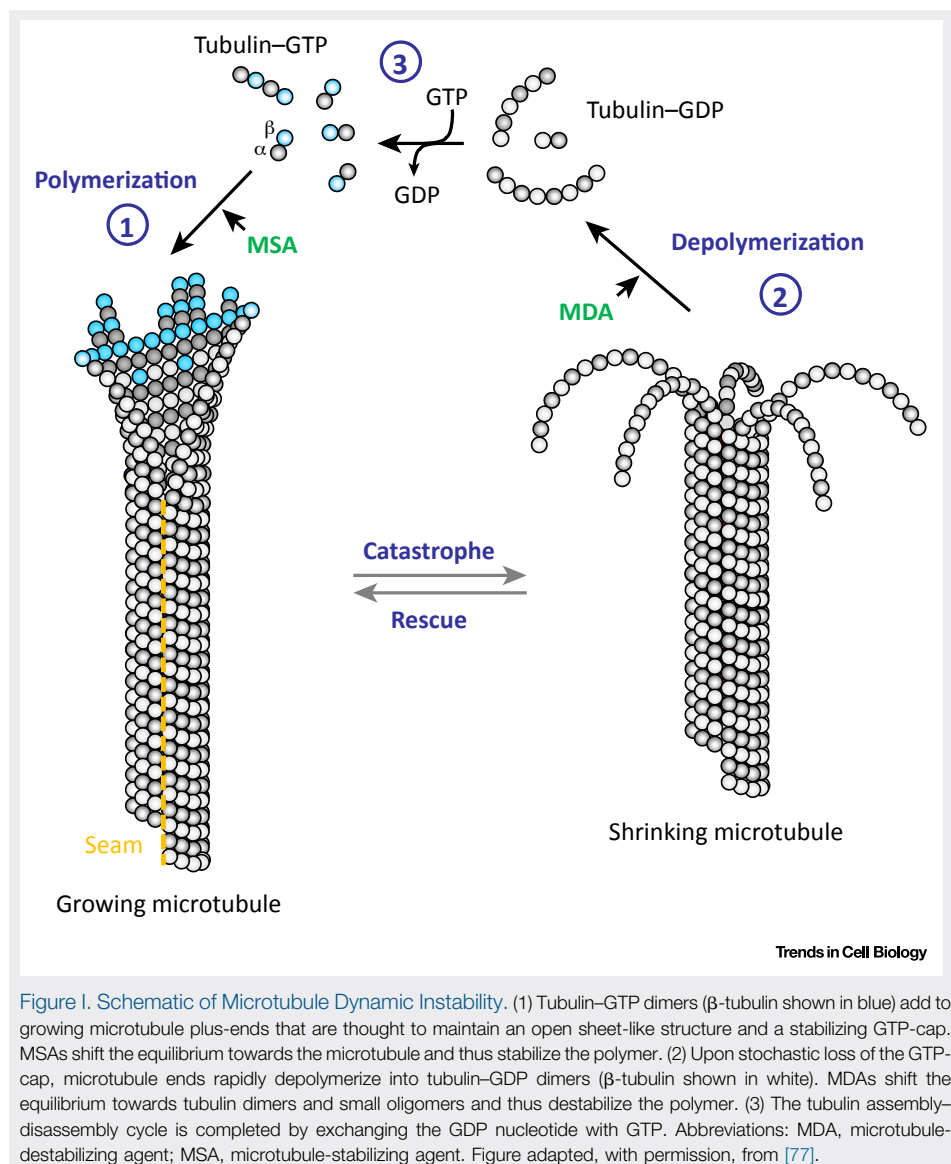


Figure 1. Schematic of Microtubule Dynamic Instability. (1) Tubulin-GTP dimers (β -tubulin shown in blue) add to growing microtubule plus-ends that are thought to maintain an open sheet-like structure and a stabilizing GTP-cap. MSAs shift the equilibrium towards the microtubule and thus stabilize the polymer. (2) Upon stochastic loss of the GTP-cap, microtubule ends rapidly depolymerize into tubulin-GDP dimers (β -tubulin shown in white). MDAs shift the equilibrium towards tubulin dimers and small oligomers and thus destabilize the polymer. (3) The tubulin assembly-disassembly cycle is completed by exchanging the GDP nucleotide with GTP. Abbreviations: MDA, microtubule-destabilizing agent; MSA, microtubule-stabilizing agent. Figure adapted, with permission, from [77].

the density of electrons of the macromolecules within the crystal. **X-ray free-electron laser:** ultra-high-energy X-ray laser consisting of ultra-high-speed electrons moving freely through a magnetic structure. The methods can be used to perform, for example, time-resolved crystallography experiments.

elucidation of taxane-site MSAs bound to tubulin to high resolution, including epothilone, zampanolide, discodermolide, and taccalonolide (Table 1). All these agents bind to a pocket of β -tubulin located on the luminal side of microtubules, which is denoted the taxane site (Figure 2A–D). The taxane site is predominantly formed by hydrophobic residues of helix H7, strand S7, and loops H6–H7, S7–H9 (the M-loop), and S9–S10 of β -tubulin. All taxane-site ligands establish both hydrophobic and polar contacts with several of these secondary structural elements. Notably, zampanolide and taccalonolide AJ (a variant of the taccalonolide family of compounds) are covalently bound to His229 and Asp226, respectively [11,12].

While taccalonolide AJ displaces the M-loop into a more open conformation that is prone to establish lateral contacts in microtubules [11], the most striking feature observed in the crystal structures of zampanolide, epothilone A, and the discodermolide–paclitaxel hybrid KS-1-199-32

Table 1. Tubulin/Microtubule–MTA complex Structures Ordered by Binding Site.

PDB ^a ID	System ^b	Ligand	Experimental method	Resolution (Å)	Refs
Microtubule-stabilizing agents					
Taxane site					
5MF4	T2R-TTL ^c	Dictyostatin	X-ray ^d	2.3	[78]
5LXT	T2R-TTL	Discodermolide	X-ray	1.9	[13]
1TVK	Zinc-sheets ^e	Epothilone A	EC ^f	2.9	[79]
4I50	T2R-TTL	Epothilone A	X-ray	2.3	[12]
4O4I	T2R-TTL	Epothilone A/laulimalide ^l	X-ray	2.4	[22]
4O4L	T2R-TTL	Epothilone A/peloruside A ^l	X-ray	2.2	[22]
5W3H	Yeast MT ^g	Epothilone B	Cryo-EM ^h	4.0	[80]
5LXS	T2R-TTL	KS-1-199-32	X-ray	2.2	[13]
5EZY	T2R-TTL	Taccalonolide AJ	X-ray	2.1	[11]
1JFF	Zinc-sheets	Taxol	EC	3.5	[9,10]
3J6G	MT	Taxol	Cryo-EM	5.5	[14]
5SYF	MT	Taxol	Cryo-EM	3.5	[15]
5W3J	Yeast MT	Taxol	Cryo-EM	4.0	[80]
5SYE	MT	Taxol/peloruside A ^l	Cryo-EM	3.5	[15]
4I4T	T2R-TTL	Zampanolide	X-ray	1.8	[12]
5SYG	MT	Zampanolide	Cryo-EM	3.5	[15]
5NG1	T2R-TTL	Zampanolide/MTC ^l	X-ray	2.2	[18]
Laulimalide/peloruside site					
4O4H	T2R-TTL	Laulimalide	X-ray	2.1	[22]
4O4I	T2R-TTL	Laulimalide/epothilone A ^l	X-ray	2.4	[22]
4O4J	T2R-TTL	Peloruside A	X-ray	2.2	[22]
5SYC	MT	Peloruside A	Cryo-EM	3.5	[15]
4O4L	T2R-TTL	Peloruside A/epothilone A ^l	X-ray	2.2	[22]
5SYE	MT	Peloruside A/taxol ^l	Cryo-EM	3.5	[15]
Microtubule-destabilizing agents					
Colchicine site					
5GON	T2R-TTL	β-Lactam bridged CA-4 analog 9	X-ray	2.5	[81]
5XLT	T2R-TTL	4'-Demethylepipodophyllotoxin	X-ray	2.8	[82]
5OSK	T2R-TTL	7j	X-ray	2.1	[83]
5YL4	T2R-TTL	8WR	X-ray	2.6	[84]
3HKC	T2R ⁱ	ABT751	X-ray	3.8	[24]
4Q2A	T2R-TTL	BAL27862	X-ray	2.5	[85]
5M7E	T2R-TTL	BKM120	X-ray	2.1	[63]
1SA0	T2R	Colchicine	X-ray	3.6	[23]
4Q2B	T2R-TTL	Colchicine	X-ray	2.3	[85]
5EYP	T-DARPin ^j	Colchicine	X-ray	1.9	[86]
5NM5	T-DARPin	Colchicine	X-ray (RT SMX ^k)	2.1	[87]
3DU7	T2R	Colchicine/phomopsisin A ^l	X-ray	4.1	[32]

Table 1. (continued)

PDB ^a ID	System ^b	Ligand	Experimental method	Resolution (Å)	Refs
3E22	T2R	Colchicine/soblidotin ^l	X-ray	3.8	[32]
3UT5	T2R	Colchicine/ustiloxin ^l	X-ray	2.7	[35]
1Z2B	T2R	Colchicine/vinblastine ^l	X-ray	4.1	[34]
5LYJ	T2R-TTL	Combretastatin A4	X-ray	2.4	[88]
4YJ3	T2R-TTL	Compound 2	X-ray	3.8	[89]
5XAF	T2R-TTL	Compound Z1	X-ray	2.6	[90]
5XAG	T2R-TTL	Compound Z2	X-ray	2.6	[90]
5H7O	T2R-TTL	DJ-101	X-ray	2.8	[91]
5CA0	T2R-TTL	Lexibulin	X-ray	2.5	[92]
4YJ2	T2R-TTL	MI-181	X-ray	2.6	[89]
5NFZ	T2R-TTL	MTC	X-ray	2.1	[18]
5NG1	T2R-TTL	MTC/zampanolide ^l	X-ray	2.2	[18]
5M7G	T2R-TTL	MTD147	X-ray	2.3	[63]
5M8G	T2R-TTL	MTD265	X-ray	2.2	[63]
5M8D	T2R-TTL	MTD265-R1	X-ray	2.3	[63]
5CA1	T2R-TTL	Nocodazole	X-ray	2.4	[92]
3N2K	T2R	NSC 613862	X-ray	4.0	[93]
3N2G	T2R	NSC 613863	X-ray	4.0	[93]
5C8Y	T2R-TTL	Plinabulin	X-ray	2.6	[92]
5XHC	T2R-TTL	PO10	X-ray	2.8	TBP ^m
5X15	T2R-TTL	PO5	X-ray	2.8	TBP
1SA1	T2R	Podophyllotoxin	X-ray	4.2	[23]
5OV7	T2R-TTL	Rigosertib	X-ray	2.4	[94]
3HKE	T2R	T138067	X-ray	3.6	[24]
5LP6	T2R-TTL	Thiocolchicine	X-ray	2.9	[95]
5CB4	T2R-TTL	Tivantinib	X-ray	2.2	[92]
3HKD	T2R	TN16	X-ray	3.7	[24]
5XLZ	T2R-TTL	TPI1	X-ray	2.3	[96]
6FKL	T2R-TTL	TUB015	X-ray	2.1	[97]
6FKJ	T2R-TTL	TUB075	X-ray	2.2	[97]
5JVD	T2R-TTL	TUB092	X-ray	2.4	[98]
Vinca site					
5H74	T2R-TTL	14b	X-ray	2.6	TBP
4X1I	T2R	20a (PF06380101)	X-ray	3.1	[33]
4X1K	T2R	22a	X-ray	3.5	[33]
4X1Y	T2R	22b	X-ray	3.2	[33]
4X20	T2R	22g	X-ray	3.5	[33]
5KX5	T2R-TTL	Compound 11	X-ray	2.5	[99]
5LOV	T2R-TTL	DZ-2384	X-ray	2.4	[39]
5JH7	T2R-TTL	Eribulin	X-ray	2.3	[36]

Table 1. (continued)

PDB ^a ID	System ^b	Ligand	Experimental method	Resolution (Å)	Refs
4ZI7	T2R-TTL	HTI286	X-ray	2.5	[38]
4ZHQ	T2R-TTL	MMAE	X-ray	2.6	[38]
5IYZ	T2R-TTL	MMAE	X-ray	1.8	[37]
5J2U	T2R-TTL	MMAF	X-ray	2.5	[37]
3DU7	T2R	Phomopsin A/colchicine ^l	X-ray	4.1	[32]
3E22	T2R	Soblidotin/colchicine ^l	X-ray	3.8	[32]
5NJH	T2R-TTL	Triazolopyrimidine-1	X-ray	2.4	[100]
4ZOL	T2R-TTL	Tubulysin M	X-ray	2.5	[38]
3UT5	T2R	Ustiloxin/colchicine ^l	X-ray	2.7	[35]
4EB6	T2R	Vinblastine	X-ray	3.5	[35]
5BMV	T2R-TTL	Vinblastine	X-ray	2.5	[38]
5J2T	T2R-TTL	Vinblastine	X-ray	2.2	[37]
1Z2B	T2R	Vinblastine/colchicine ^l	X-ray	4.1	[34]
Maytansine site					
6FJM	T2R-TTL	Disorazole Z	X-ray	2.4	[49]
4TV8	T2R-TTL	Maytansine	X-ray	2.1	[48]
4TV9	T2R-TTL	PM060184	X-ray	2.0	[48]
4TUY	T2R-TTL	Rhizoxin	X-ray	2.1	[48]
6FII	T2R-TTL	Spongistatin	X-ray	2.1	[49]
Pironetin site					
5FNV	T2R-TTL	Pironetin	X-ray	2.6	[57]
5LA6	T2R-TTL	Pironetin	X-ray	2.1	[58]

^aPDB, Protein Data Bank.

^bSystem, tubulin assembly to which the ligand was bound.

^cT2R-TTL, tubulin:RB3:TTL complex (TTL, tubulin tyrosine ligase; RB3, stathmin-like domain of rat stathmin-like protein B3).

^dX-ray, X-ray crystallography.

^eZinc-sheets, zinc-stabilized sheets of tubulin.

^fEC, electron crystallography.

^gMT, microtubule.

^hCryo-EM, cryogenic electron microscopy.

ⁱT2R, tubulin:RB3 complex.

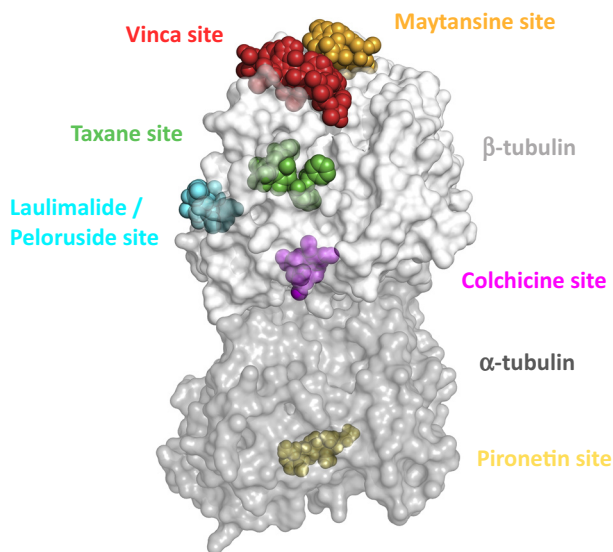
^jT-DARPin, tubulin:designed ankyrin repeat protein complex.

^kRT SMX, room-temperature serial millisecond crystallography.

^lBinary complexes are listed twice.

^mTBP, to be published.

in complex with tubulin is the structuring of the otherwise disordered M-loop into a short helix, which is induced by their respective sidechains [12,13]. Because the M-loop is a major element establishing lateral tubulin contacts in microtubules, this observation readily explains how taxane-site ligands promote microtubule assembly and stability (Figure 2D). The functional relevance of M-loop structuring is underpinned by the fact that its helical conformation is also observed in cryo-EM reconstructions of microtubules [14–16]: as shown in Figure 2D, the respective taxane site C α atoms of free and polymerized tubulin superimpose very well with a root-mean-square deviation (rmsd) of only 0.9 Å. This result highlights that both X-ray crystallography and cryo-EM can be used in a complementary manner to investigate the molecular mechanism of action of MSAs in great detail.



Trends in Cell Biology

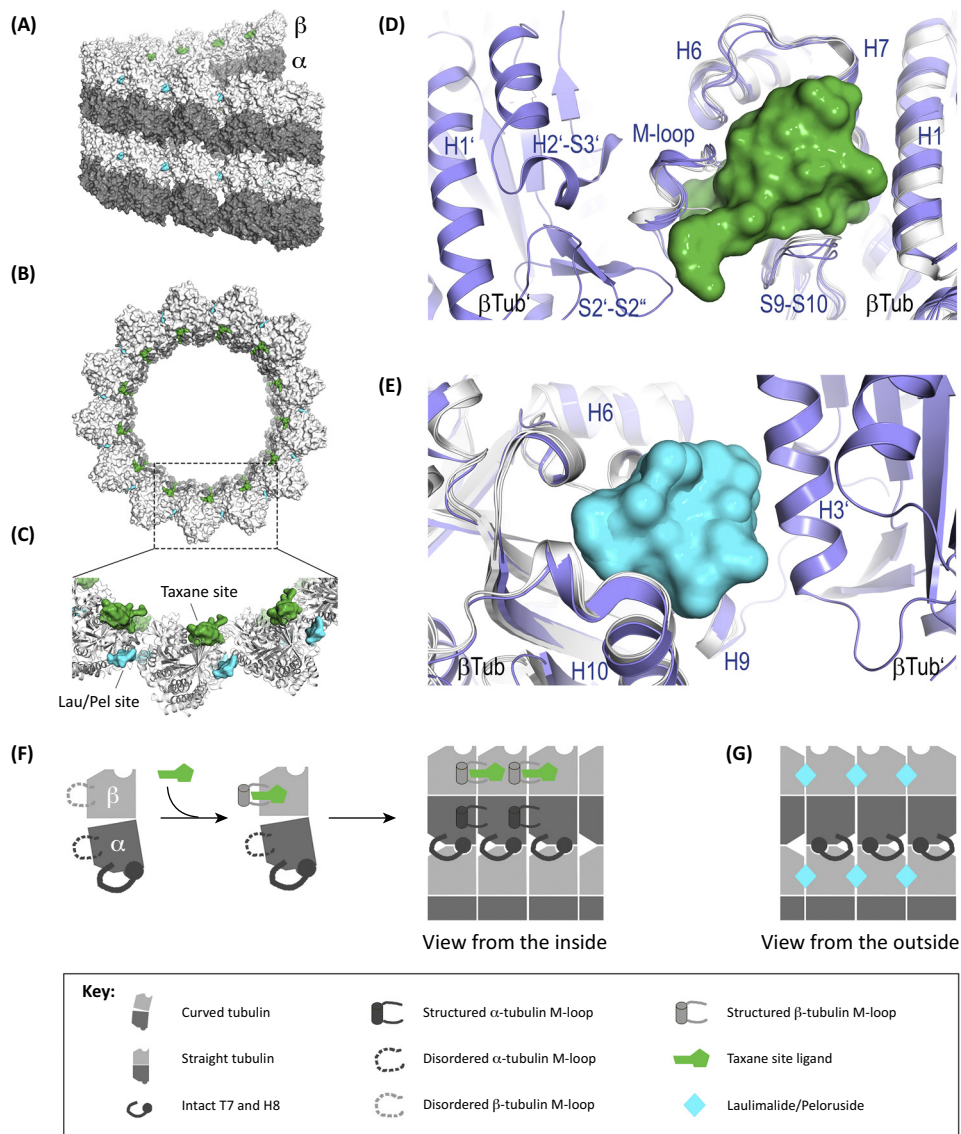
Figure 1. Microtubule-Targeting Agent (MTA) Binding Sites on Tubulin. The $\alpha\beta$ -tubulin dimer (α - and β -tubulin in dark and in light grey, respectively) with bound ligands is shown in semitransparent surface representation. The structures of representative ligands for each site were superimposed onto their respective binding sites. To highlight the distinct binding sites, all ligands are shown in sphere representation and are colored in green (taxane site), cyan (laulimalide/peloruside site), magenta (colchicine site), slate (vinca site), orange (maytansine site), or yellow (pironetin site).

Notably, paclitaxel, taccalonolide, and discodermolide do not possess a sidechain that engages with the M-loop, whereas zampanolide, epothilone A, and KS-1-199-32 do [11,13,14]. Atomic force and cryo-EM studies suggest that paclitaxel stabilizes microtubules by strengthening longitudinal tubulin contacts via an **allosteric** mechanism [14,17]. An allosteric effect has also been proposed for taccalonolide AJ and zampanolide, which upon binding to the taxane site inhibit hydrolysis or reduce the affinity, respectively, of the remotely located GTP nucleotide on β -tubulin [11,18]. Collectively, these observations suggest that different taxane-site ligands, although binding to the same pocket on β -tubulin, may achieve their microtubule-stabilizing effect through different molecular mechanisms. The taxane site could thus be considered as an ensemble of functionally diverse subsites whose differential occupation by a ligand elicits different conformational effects in tubulin within the microtubule lattice.

Laulimalide and Peloruside A

Laulimalide and peloruside A are potent MSAs isolated from the marine sponges *Mycale hentscheli* and *Cacospongia mycofijiensis*, respectively [19,20]. Both compounds exhibit significant cytotoxic activity against a broad range of cancer cell lines and have unique features compared to taxane-site ligands used in the clinics [21]. Recently, high-resolution X-ray crystallography and cryo-EM studies allowed the description of the laulimalide/peloruside site on β -tubulin, which is distinct from the taxane site [15,22]. Compared to the taxane site, that is located at the luminal side of the microtubule, the common pocket on β -tubulin that is targeted by both laulimalide and peloruside A faces the outside of the microtubule (Figure 2A–C).

The laulimalide/peloruside site is formed by hydrophobic and polar residues of helices H9 and H10, and the loops H9–H9' and H10–S9 of β -tubulin. It is positioned near the lateral interface between protofilaments on the outer surface of the microtubule (Figure 2E). Both ligands could in principle establish lateral contacts with helix H3 of the juxtaposed tubulin subunit in the



Trends in Cell Biology

Figure 2. Binding Modes and Molecular Mechanisms of Action of Microtubule-Stabilizing Agents (MSAs).

Side (A) and top (B) views of a microtubule with taxane-site (green) and laulimalide/peloruside-site (cyan) ligands. α - and β -tubulin subunits are shown in light- and dark-grey surface representations, respectively. (C) Close-up view of the boxed area in (B). (D) Superimposed taxane sites in the curved and straight tubulin conformational states. For simplicity, only one representative tubulin structure is shown. β Tub and β Tub' indicate β -tubulin subunits that belong to two neighboring protofilaments, respectively. The superposition highlights that both the helical conformation and orientation of the M-loop seen in crystal structures of tubulin–ligand complexes are very similar to those observed in cryo-electron microscopy reconstructions of native microtubules. (E) Superimposed laulimalide/peloruside (Lau/Pel) sites in the curved and straight tubulin conformational states. The superimposed ligands are shown in cyan. (F) Schematic representation of the mechanism of action of taxane-site MSAs on tubulin and microtubules. Binding of a ligand induces the structuring of the otherwise disordered M-loop of β -tubulin into a short helix. The thus-stabilized M-loop promotes tubulin assembly into a microtubule, where the α -tubulin M-loops also adopt a helical conformation. In the absence of a taxane-site ligand the M-loop helix of β -tubulin is also formed in the context of the microtubule. (G) Schematic representation of the molecular mechanism of action of laulimalide and peloruside A. The MSAs bind at the interface between two adjacent β -tubulin subunits and may act as a 'clamp' to strengthen interactions across protofilaments in the microtubule.

adjacent protofilament, and may thus inhibit microtubule disassembly by acting as molecular ‘clamps’ that hold together protofilaments (Figure 2E). Interestingly, cryo-EM studies revealed that peloruside A has a particular pronounced effect on lateral tubulin contacts at the **microtubule lattice seam**, a well-known discontinuity in the microtubule lattice [15] (Box 1). In addition, laulimalide or peloruside A binding to β -tubulin also stabilizes structural elements in the proximity of the M-loop, thereby providing an allosteric contribution to M-loop-mediated lateral contacts in microtubules [22]. Because the M-loop is an element of the taxane site (see above), these results indicate a biochemical crosstalk between the laulimalide/peloruside and taxane site, a hypothesis that remains to be proven.

Tubulin-Binding and Molecular Mechanisms of Action of MDAs

Colchicine-Site Ligands

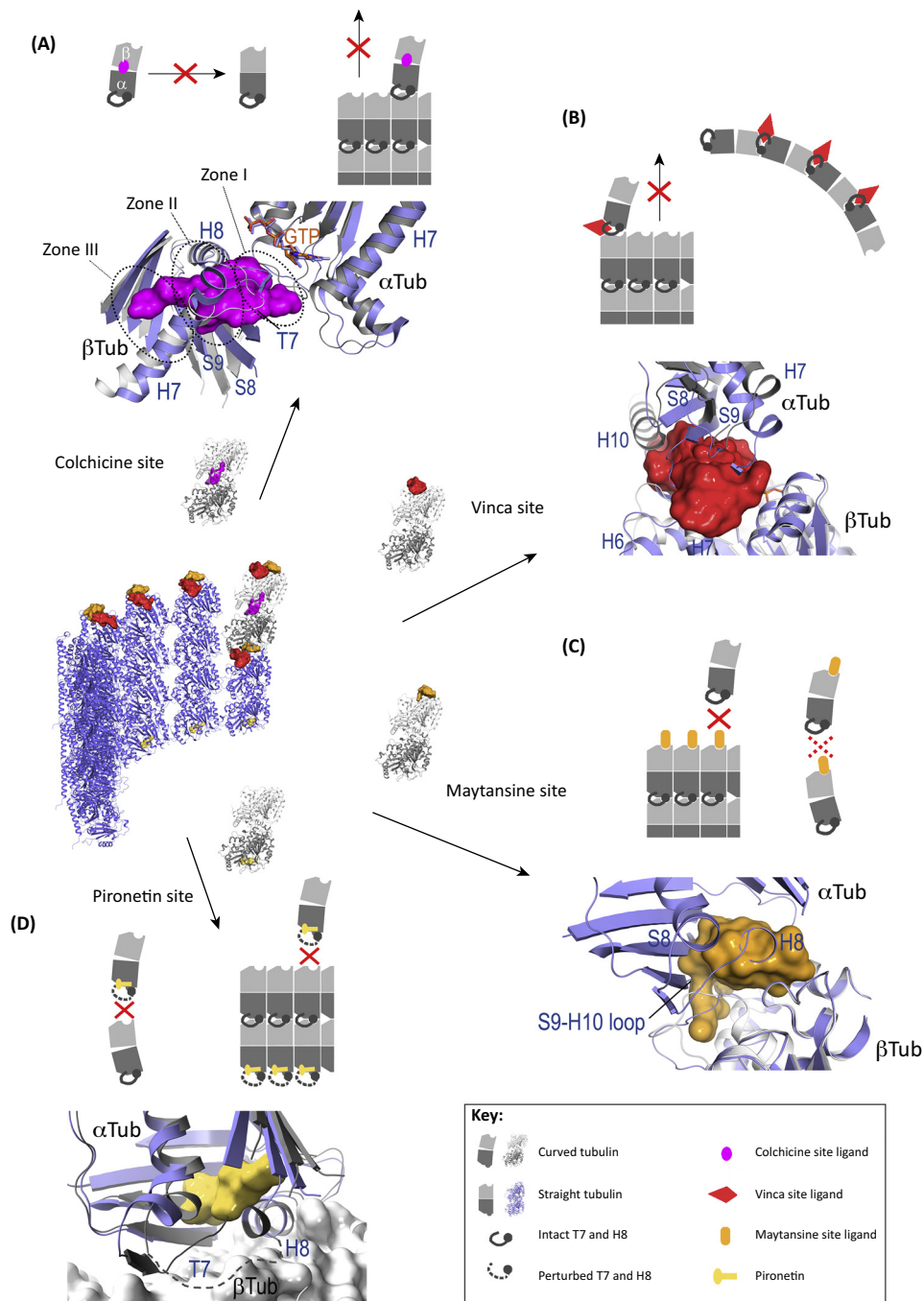
Colchicine-site ligands are probably the most extensively studied class of MTAs; however, none of them have reached the commercial phase yet. Since the first atomic description of colchicine binding to tubulin in 2004 [23], a large number of structurally diverse colchicine-site ligands of natural or synthetic origin in complex with tubulin have been characterized by X-ray crystallography to medium and high resolution (Table 1).

The colchicine site is a deep pocket mostly buried in the intermediate domain of β -tubulin [9,10], which is located near the intra-dimer interface between the α - and β -tubulin subunits [23,24]. It is shaped by helices H7 and H8, the T7 loop, and the S8 and S9 strands of β -tubulin, and is completed by the T5 loop of α -tubulin (Figure 3A). The site can be subdivided into a main zone in the center of the domain (zone 2) and two additional accessory pockets that either face the α -tubulin subunit (zone 1) or are buried deeper in the β -tubulin subunit (zone 3; Figure 3A) [25]. The colchicine-site ligands that have been structurally characterized so far cluster either in zones 1 and 2, or zones 2 and 3, but no ligand that occupies all three zones simultaneously has been described [26].

In the bound state, all the core secondary structural elements of the colchicine site interact with the ligand through mainly hydrophobic and very few polar contacts. The main feature observed upon ligand binding is a switch of the T7 loop that is needed to free up the space to allow the ligand to bind. In the course of microtubule assembly, tubulin dimers undergo conformational changes from a ‘curved’ conformation in their free state [23] to a ‘straight’ structure in microtubules ([9,10]; reviewed in [3]). The ‘curved-to-straight’ conformational transition is characterized by movement of the intermediate domain of both α - and β -tubulin subunits, in which strands S8 and S9, among others, move closer to helix H8. These conformational changes are accompanied by a translation of helix H7 and lead to an overall contraction of the colchicine site [23,24]. Thus, binding of a ligand to the colchicine site inhibits microtubule formation mainly by preventing the curved-to-straight conformational change in tubulin (Figure 3A).

Vinca-Site Ligands

The vinca alkaloids represent the oldest family of compounds that target the vinca site of tubulin. Since the first description of antitumor activity of this class of compounds in the late 1950s, vinblastine and vincristine have received extensive clinical evaluation, proving effective against a variety of malignancies [27]. The vinca site-targeting agents known to date comprise several chemical classes of compounds of both natural and synthetic origin, such as the highly potent cytotoxic peptides dolastatins, auristatins, and tubulysins which are used as payloads for ADCs, as well as eribulin, diazonamides, and triazolopyrimidines [28–31] (Table 1).



Trends in Cell Biology

Figure 3. Binding Modes and Molecular Mechanisms of Action of Microtubule-Destabilizing Agents (MDAs).

(A) Colchicine-site MDAs destabilize microtubules by preventing the curved-to-straight conformational transition in the α - β -tubulin heterodimer. (B) Vinca-site MDAs destabilize microtubules by introducing a wedge at the interface between two longitudinally aligned tubulin dimers at the tips of microtubules, or by stabilizing assembly-incompetent ring-like oligomers. (C) Maytansine-site ligands destabilize microtubules by binding to β -tubulin (β Tub) and inhibiting longitudinal tubulin-tubulin interactions. However, under conditions of Mg^{2+} -induced tubulin self-association, some maytansine-site ligands can induce ring-like tubulin oligomer formation. (D) Pironetin destabilizes microtubules by binding to and perturbing helix

(Figure legend continued on the bottom of the next page.)

Ligands targeting the vinca site bind at the inter-dimer interface between two longitudinally aligned tubulin dimers (Figure 3B). The vinca site consists of a core zone, which has been defined based on interactions established by vinca alkaloids, and a pocket that extends towards the exchangeable guanosine nucleotide site on β -tubulin [32,33]. The secondary structural elements of the core zone comprise the C-terminal turn of helix H6, loops T5 and H6–H7 of β 1-tubulin, and helix H10, strand S9, and loop T7 of α 2-tubulin [34,35]. Ligands that elongate beyond the core of the vinca site form more extensive interactions with the β 1-tubulin H6–H7 loop and helix H7, and with the β -tubulin-bound nucleotide, thereby inhibiting its exchange [36–38]. Recently, allosteric crosstalk between peptidic vinca-site ligands carrying terminal carboxylate residues and the M-loop was proposed as an additional stabilizing mechanism to maintain the M-loop in an incompatible conformation for productive lateral tubulin contact formation in microtubules [37].

Microtubule destabilization by vinca-site ligands is achieved either by introducing a molecular ‘wedge’ at the tip of microtubules, which prevents the curved-to-straight transition of tubulin necessary for proper incorporation into microtubules (see above), or by sequestering tubulin dimers into ring-like oligomers that are incompatible with the straight protofilament structure in microtubules (Figure 3B). Ligand binding further inhibits proper positioning of the catalytic α -tubulin residues that promote GTP-hydrolysis on β -tubulin [34,35]. Interestingly, the vinca-site ligand DZ-2384 causes straightening of curved protofilaments [39], suggesting that the degree of curvature of longitudinally aligned tubulin dimers can be modulated by the different types of vinca-site ligands.

Maytansine-Site Ligands

The maytansine derivative DM1 is part of the ADC trastuzumab emtansine, which is currently in clinical use for the treatment of metastatic breast cancer [40]. Canonical maytansine-site ligands have been known to interfere with vinblastine binding to tubulin, but the location of their exact binding site has long been a matter of debate [41–43]. It was X-ray crystallography that clarified this issue recently by solving the structures of the unrelated MDAs rhizoxin [44], maytansine [40], PM60184 [45], spongistatin [46], and disorazole [47] in complex with tubulin [48,49] (Table 1).

The maytansine site is distinct from the vinca site and is located on an exposed pocket of β -tubulin, which accommodates loop H10–S9, strand S8, and helix H8 of α -tubulin at the longitudinal tubulin interface in microtubules (Figure 3C). It is located adjacent to the guanosine nucleotide and is shaped by hydrophobic and polar residues of helices H3', H11, and H11', as well as the loops S3–H3' (T3-loop), S5–H5 (T5-loop), and H11–H11' of β -tubulin [48]. In the context of ‘straight’ tubulin, the overall shape of this pocket is invariant, suggesting that the ligands bind independently of the conformational state of tubulin [48]. This observation implies that maytansine-site ligands directly block the formation of longitudinal tubulin contacts in microtubules either by inhibiting the addition of further tubulin dimers to the **plus ends** of growing microtubules, or by forming assembly incompetent tubulin–ligand complexes at high ligand concentrations (Figure 3C). Under conditions of elevated concentrations of magnesium ions, some maytansine-site ligands such as PM60184 variants were shown to also induce tubulin ring-like oligomers [42].

H8 and loop T7 of α -tubulin (α Tub), which inhibits longitudinal tubulin–tubulin interactions. In each panel the schematic mechanism of action of a class of MDA and the superimposition of the respective binding site in the curved (grey ribbon) and straight (slate ribbon) tubulin conformational states are shown at the top and bottom, respectively. A summarizing ribbon representation of a piece of a microtubule with all superimposed ligand-binding sites and a curved tubulin dimer is shown at the center left of the figure.

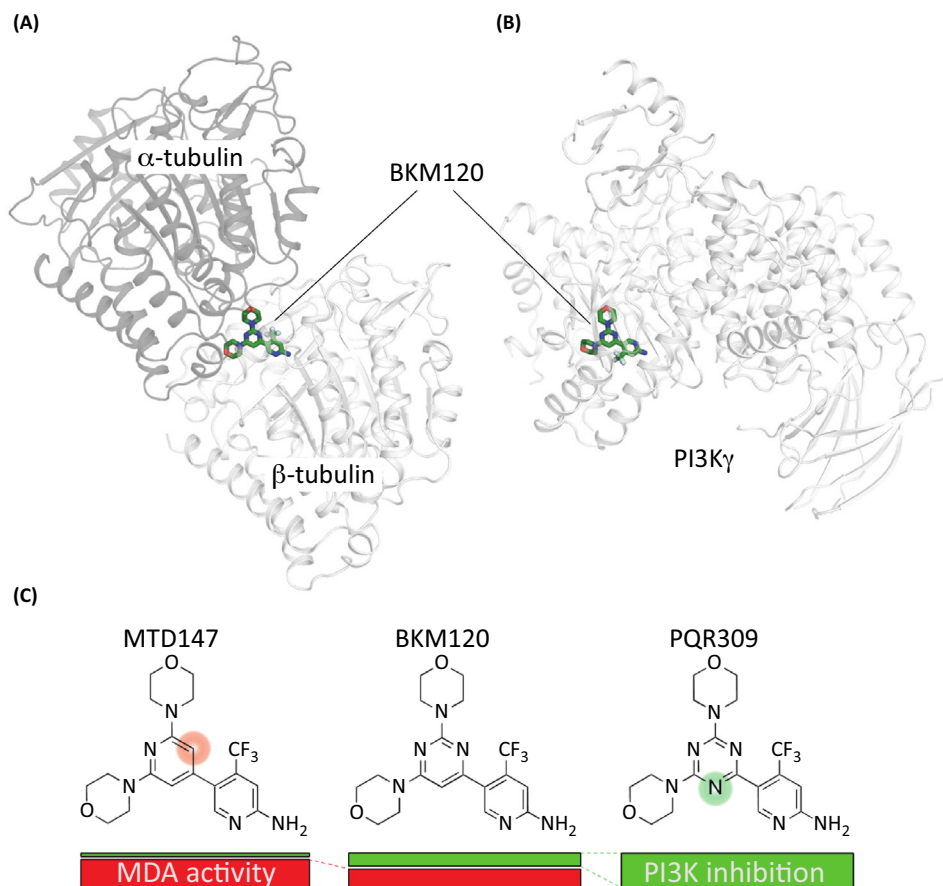
Pironetin

Pironetin was first extracted from fermentation broths of *Streptomyces* strains as a plant growth regulator [50,51], and was later reported to show antimitotic and antitumor activity by inhibiting microtubule formation [52,53]. A covalent-binding mechanism of action of pironetin was proposed based on structure–activity relationship studies [54]. Subsequently, Lys352 of α -tubulin was identified as the pironetin-binding site by systematic alanine-scanning mutagenesis [55]. Using this information in combination with molecular dynamics simulations, it has been further speculated that pironetin destabilizes microtubules by perturbing the formation of lateral tubulin contacts in microtubules [56]. However, two recent independent X-ray crystallography studies reported the covalent binding of pironetin to Cys316 of α -tubulin [57,58]. The ligand binds to an extended hydrophobic pocket on α -tubulin, with its pyrone ring interacting with residues of strands S8 and S10, and with helix H7 (Figure 3D). The sidechain of pironetin is further buried in a pocket shaped by residues belonging to helix H7 and by strands S4, S5, and S6. This binding mode causes a disorder of the T7 loop and a conformational perturbation in the N-terminal section of helix H8 of α -tubulin. Because these two secondary structural elements establish key longitudinal tubulin contacts along protofilaments in microtubules, it was proposed that their perturbation can prevent microtubule formation either at high ligand concentrations by forming assembly incompetent tubulin–pironetin complexes, or at substoichiometric compound concentrations by inhibiting the addition of further tubulin dimers at the **minus ends** of microtubules that expose α -tubulin subunits (Figure 3D) [58]. Notably, pironetin is the only known compound to date that exclusively targets the α -tubulin subunit.

Kinase Inhibitors that Target Microtubules

As mentioned earlier, MTAs are very diverse both in terms of chemical structures and molecular weights. Furthermore, some binding pockets on tubulin, such as the colchicine and the taxane sites, are fairly deep, large in size, and predominantly hydrophobic in nature. It is thus not surprising that several different types of anticancer drugs that were initially developed against other protein targets such as, for example, kinases turned out to also bind tubulin and to display off-target effects [59]. Kinases are enzymes that phosphorylate proteins at specific amino acid sites, and malfunctioning of kinases is often linked to cell transformation. Because both kinase and tubulin anticancer drugs promote cell-cycle arrest and exhibit antiproliferative activities, it is often not straightforward to identify their exact modes of action by phenotypic analyses alone. However, the availability of such information is crucial to correctly interpret pharmacological and clinical data in the context of side-effect evaluations or the determination of toxicity mechanisms. In the following section we briefly discuss one example of a compound that was initially developed against a kinase, but which was subsequently demonstrated by thorough chemical, structural, and functional analyses to bind to tubulin and affect microtubule dynamics. For a more comprehensive overview of dual kinase/tubulin inhibitors we refer to a recent review [59].

BKM120 (buparlisib, NVP-BKM120) is one of the most advanced phosphoinositide 3-kinase (PI3K) inhibitors enlisted in more than 80 clinical studies as a single drug or in combination chemotherapies. The compound has excellent pharmacological properties, is highly selective for the class I PI3Ks, and is one of the few PI3K inhibitors that readily cross the blood–brain barrier [60,61]. However, in addition to inhibiting class I PI3Ks, BKM120 has also been reported to interact with tubulin and to destabilize microtubules *in vitro* and in cells as an off-target effect [62]. The tubulin- and PI3K-binding modes of several BKM120 derivatives have been investigated by X-ray crystallography, and this provided detailed insight into the selectivity mechanism of the drug [60,63]. It was found that the ligand binds both to the colchicine site of tubulin as well



Trends in Cell Biology

Figure 4. Dual Inhibition of Tubulin and PI3K by BKM120. (A,B) X-ray crystal structures of tubulin–BKM120 (PDB 5M7E) and PI3K γ –BKM120 (PDB 3SD5) complexes, respectively. α -Tubulin, β -tubulin, and PI3K γ are shown in transparent ribbon representations. The BKM120 molecules in both protein structures, which were aligned with respect to each other, are shown in green sticks representation. (C) Exchange of the pyrimidine core with either pyridine or triazine in BKM120 yields the specific microtubule-destabilizing agent (MDA) MTD147 or the specific PI3K inhibitor PQR309, respectively. Filled boxes below the chemical structures indicate the degree of MDA (red) and PI3K (green) inhibitor activities. Figure adapted, with permission, from [63].

as to the ATP site of PI3K (Figure 4AB), and that its antiproliferative activity is mainly due to microtubule disruption rather than to PI3K inhibition [63]. Strikingly, a minute change of one Dalton in the pyrimidine core of the BKM120 molecule separated its dual activity into discrete PI3K and tubulin inhibition (Figure 4C) [63].

The example of BKM120 demonstrates the power of combinatorial chemistry, cell biology, biochemistry, and structural biology approaches to identify the physiologically relevant target of a small molecule. The results obtained on this compound further showcase how high-resolution structural information can be used to improve target specificity and thus the safety profile of next-generation agents to be developed and used in single and combination chemotherapies. The steadily increasing list of cytotoxic agents that were initially designed against a kinase, but which then turned out to interfere with microtubule dynamics [59], highlights that tubulin should be considered as a possible molecular off-target during the early stages of cytotoxic drug development.

Concluding Remarks and Future Perspectives

Recent breakthroughs in the tubulin structural biology field have enabled the discovery and detailed characterization of new ligand-binding sites on tubulin and deciphering the molecular mechanisms of action of a large number of MTAs. While both X-ray crystallography and cryo-EM provide detailed, albeit static, views of tubulin/microtubule–MTA interactions, acquiring information on how ligands affect the functionally crucial dynamics of the $\alpha\beta$ -tubulin heterodimer as well as of the shaft and ends of a microtubule remains a challenge. The availability of such knowledge may help us to understand how exactly chemically and structurally completely different molecules targeting the same binding site on tubulin, for example taxane-site ligands, elicit their actual effect. In this context, the massive amount of high-resolution structural information that has become available over the past ~ 5 years (Table 1), and which very likely will further increase in the coming years, offers a unique resource for systematic molecular dynamics simulations to address this important question. On the other hand, cryo-electron tomography in combination with novel image-analysis approaches or high-speed atomic force microscopy in the absence and presence of low and clinically relevant concentrations of MTAs may provide the means to experimentally assess in detail the conformational effects elicited by MTAs on growing and shrinking microtubule tips.

It is interesting to note that five of the six currently known MTA binding sites reside on β -tubulin (Figure 1). A possible reason for this bias could be that the GTP hydrolysis cycle that is necessary for driving microtubule dynamic instability takes place on β -tubulin (Box 1), and that ligands targeting this particular tubulin subunit could somehow interfere with this functionally crucial process. In this context, it is actually surprising that no ligand has yet been found that binds to the nucleotide site on β -tubulin – this would be a direct and effective strategy to disrupt microtubule dynamics. A more general and intriguing question along these lines is whether additional binding sites, in particular on α -tubulin, exist in addition to the six known today (see Outstanding Questions). The different crystallization tools that have been recently developed for tubulin [12,64–66], in combination with the huge advances in highly automated and fast X-ray data collection and processing technologies at **synchrotrons**, will allow the screening of thousands of small molecules including chemical fragments [67] to address this intriguing question.

The human genome harbors several α - and β -tubulin genes and thus different tubulin isotypes (reviewed in [7]). Furthermore, the $\alpha\beta$ -tubulin heterodimer can be post-translationally modified by a set of enzymes, including polyglutamylation, polyglycylation, acetylation, and deetyrosination (reviewed in [68]). It is poorly understood at a mechanistic level how this variety of residue substitutions and modifications affect the action of MTAs on tubulin and microtubules. In this context, recent advances in recombinant tubulin technologies [69,70] should provide unique opportunities to systematically address this important problem and perhaps even allow, for example, the rational development of a range of different tubulin isotype-specific MTAs. It is well known that one important resistance mechanism that emerges in all chemotherapies employing MTAs is the upregulation of specific tubulin isotypes by cancer cells, in particular $\beta 3$ -tubulin. The availability of tubulin isotype-specific compounds would thus not only help to circumvent an important resistance mechanism during antitubulin chemotherapy but also provide tools to target specific microtubule subtypes in cells and tissues.

The applications of MTAs in cell biology research as well as oncology have been so far limited to the treatment of entire cell populations. An approach to target single cells or tissues would be the development of MTAs that can be reversibly activated with high spatial and temporal resolution. Photostatins are combretastatin A-4-derived colchicine-site MTAs that can be activated and inactivated by violet and green light, respectively [71]. As such, photostatins

Outstanding Questions

How many ligand-binding sites are present on the $\alpha\beta$ -tubulin heterodimer?

Why do most MTAs bind to β -tubulin?

How do MTAs affect the conformational dynamics of the $\alpha\beta$ -tubulin heterodimer in its free form and when incorporated into microtubule tips and lattices?

How do MTAs affect the structure of microtubule ends at low concentrations?

Are there ligands that bind to the nucleotide site of β -tubulin?

Can we develop robust recombinant protein technologies to produce any tubulin isotype or mutant for biochemical, biophysical, and structural biology studies?

Can we develop model systems to better analyze the interactions of MTAs with different types of microtubules in living cells and tissues?

Is it possible to develop tubulin isotype-specific compounds?

Is it possible to engineer MTAs that are or become activated only in a tumor?

have already been shown to be useful in perturbing the microtubule cytoskeleton in single *C. elegans* cells [71]. In the context of cancer treatment, activation by visible light is not an option because it is strongly limited by the depth of the targeted tissue; modifying photostatins in a manner that they can be activated, for example, by IR light [72] may help to circumvent this problem. At a more fundamental, biochemical level, photostatins could be used to perform time resolved **X-ray free-electron laser** experiments [73] to monitor the process of ligand binding and unbinding as well as to selectively assess the accompanying dynamic structural changes occurring in tubulin.

In conclusion, MTAs remain highly valuable and interesting compounds to investigate and manipulate microtubule networks as well as important cytotoxic drugs for treating different types of severe human diseases. We expect that they will continue telling us exciting stories about microtubule structure and dynamics [74], a puzzle that deserves ongoing investigation.

Acknowledgments

M.O.S. is supported by a grant from the Swiss National Science Foundation (31003A_166608).

References

- Kueh, H.Y. and Mitchison, T.J. (2009) Structural plasticity in actin and tubulin polymer dynamics. *Science* 325, 960–963
- Bornens, M. (2012) The centrosome in cells and organisms. *Science* 335, 422–426
- Akhmanova, A. and Steinmetz, M.O. (2015) Control of microtubule organization and dynamics: two ends in the limelight. *Nat. Rev. Mol. Cell Biol.* 16, 711–726
- Dumontet, C. and Jordan, M.A. (2010) Microtubule-binding agents: a dynamic field of cancer therapeutics. *Nat. Rev. Drug Discov.* 9, 790–803
- Yang, C.H. and Horwitz, S.B. (2017) Taxol[®]: the first microtubule stabilizing agent. *Int. J. Mol. Sci.* 18, E1733
- Miltenburg, N.C. and Boogerd, W. (2014) Chemotherapy-induced neuropathy: a comprehensive survey. *Cancer Treat. Rev.* 40, 872–882
- Kavallaris, M. (2010) Microtubules and resistance to tubulin-binding agents. *Nat. Rev. Cancer* 10, 194–204
- Baas, P.W. and Ahmad, F.J. (2013) Beyond taxol: microtubule-based treatment of disease and injury of the nervous system. *Brain* 136, 2937–2951
- Nogales, E. *et al.* (1998) Structure of the alpha beta tubulin dimer by electron crystallography. *Nature* 391, 199–203
- Lowe, J. *et al.* (2001) Refined structure of alpha beta-tubulin at 3.5 Å resolution. *J. Mol. Biol.* 313, 1045–1057
- Wang, Y. *et al.* (2017) Mechanism of microtubule stabilization by taccalonolide AJ. *Nat. Commun.* 8, 15787
- Prota, A.E. *et al.* (2013) Molecular mechanism of action of microtubule-stabilizing anticancer agents. *Science* 339, 587–590
- Prota, A.E. *et al.* (2017) Structural basis of microtubule stabilization by discodermolide. *ChemBioChem* 18, 905–909
- Alushin, G.M. *et al.* (2014) High-resolution microtubule structures reveal the structural transitions in alphabeta-tubulin upon GTP hydrolysis. *Cell* 157, 1117–1129
- Kellogg, E.H. *et al.* (2017) Insights into the distinct mechanisms of action of taxane and non-taxane microtubule stabilizers from Cryo-EM structures. *J. Mol. Biol.* 429, 633–646
- Vemu, A. *et al.* (2016) Structure and dynamics of single-isoform recombinant neuronal human tubulin. *J. Biol. Chem.* 291, 12907–12915
- Elie-Caille, C. *et al.* (2007) Straight GDP-tubulin protofilaments form in the presence of taxol. *Curr. Biol.* 17, 1765–1770
- Field, J.J. *et al.* (2018) Zampanolide binding to tubulin indicates cross-talk of taxane site with colchicine and nucleotide sites. *J. Nat. Prod.* 81, 494–505
- Hood, K.A. *et al.* (2002) Peloruside A, a novel antimitotic agent with paclitaxel-like microtubule-stabilizing activity. *Cancer Res.* 62, 3356–3360
- Mooberry, S.L. *et al.* (1999) Lulimalide and isolulimalide, new paclitaxel-like microtubule-stabilizing agents. *Cancer Res.* 59, 653–660
- Kanakkanthara, A. *et al.* (2015) Beta1-tubulin mutations in the lulimalide/peloruside binding site mediate drug sensitivity by altering drug-tubulin interactions and microtubule stability. *Cancer Lett.* 365, 251–260
- Prota, A.E. *et al.* (2014) Structural basis of microtubule stabilization by lulimalide and peloruside A. *Angew. Chem. Int. Ed. Engl.* 53, 1621–1625
- Ravelli, R.B. *et al.* (2004) Insight into tubulin regulation from a complex with colchicine and a stathmin-like domain. *Nature* 428, 198–202
- Dorleans, A. *et al.* (2009) Variations in the colchicine-binding domain provide insight into the structural switch of tubulin. *Proc. Natl. Acad. Sci. U. S. A.* 106, 13775–13779
- Massarotti, A. *et al.* (2012) The tubulin colchicine domain: a molecular modeling perspective. *ChemMedChem* 7, 33–42
- Perez-Perez, M.J. *et al.* (2016) Blocking blood flow to solid tumors by destabilizing tubulin: an approach to targeting tumor growth. *J. Med. Chem.* 59, 8685–8711
- Johnson, I.S. *et al.* (1963) The vinca alkaloids: a new class of oncolytic agents. *Cancer Res.* 23, 1390–1427
- Pettit, G.R. (1997) The dolastatins. *Fortschr. Chem. Org. Naturst.* 70, 1–79
- Crowley, P.J. *et al.* (2010) Synthesis and fungicidal activity of tubulin polymerisation promoters. Part 1: pyrido[2,3-b]pyrazines. *Pest Manag. Sci.* 66, 178–185
- Jordan, M.A. *et al.* (2005) The primary antimitotic mechanism of action of the synthetic halichondrin E7389 is suppression of microtubule growth. *Mol. Cancer Ther.* 4, 1086–1095
- Lindquist, N. *et al.* (1991) Isolation and structure determination of diazonamides A and B, unusual cytotoxic metabolites from the marine ascidian *Diazona chinensis*. *J. Am. Chem. Soc.* 113, 2303–2304
- Cormier, A. *et al.* (2008) Structural insight into the inhibition of tubulin by vinca domain peptide ligands. *EMBO Rep.* 9, 1101–1106
- Maderna, A. *et al.* (2014) Discovery of cytotoxic dolastatin 10 analogues with N-terminal modifications. *J. Med. Chem.* 57, 10527–10543

34. Gigant, B. *et al.* (2005) Structural basis for the regulation of tubulin by vinblastine. *Nature* 435, 519–522
35. Ranaivoson, F.M. *et al.* (2012) Structural plasticity of tubulin assembly probed by vinca-domain ligands. *Acta Crystallogr. D Biol. Crystallogr.* 68, 927–934
36. Doodhi, H. *et al.* (2016) Termination of protofilament elongation by eribulin induces lattice defects that promote microtubule catastrophes. *Curr. Biol.* 26, 1713–1721
37. Waight, A.B. *et al.* (2016) Structural basis of Microtubule destabilization by potent auristatin anti-mitotics. *PLoS One* 11, e0160890
38. Wang, Y. *et al.* (2016) Structural insights into the pharmacophore of vinca domain inhibitors of microtubules. *Mol. Pharmacol.* 89, 233–242
39. Wiecek, M. *et al.* (2016) The synthetic diazonamide DZ-2384 has distinct effects on microtubule curvature and dynamics without neurotoxicity. *Sci. Transl. Med.* 8, 365ra159
40. Lambert, J.M. and Chari, R.V. (2014) Ado-trastuzumab emtansine (T-DM1): an antibody–drug conjugate (ADC) for HER2-positive breast cancer. *J. Med. Chem.* 57, 6949–6964
41. Mandelbaum-Shavit, F. *et al.* (1976) Binding of maytansine to rat brain tubulin. *Biochem. Biophys. Res. Commun.* 72, 47–54
42. Pera, B. *et al.* (2013) New interfacial microtubule inhibitors of marine origin, PM050489/PM060184, with potent antitumor activity and a distinct mechanism. *ACS Chem. Biol.* 8, 2084–2094
43. Takahashi, M. *et al.* (1987) Studies on macrocyclic lactone antibiotics. XI. Anti-mitotic and anti-tubulin activity of new antitumor antibiotics, rhizoxin and its homologues. *J. Antibiot.* 40, 66–72
44. Hanauske, A.R. *et al.* (1996) Phase II clinical trials with rhizoxin in breast cancer and melanoma. The EORTC Early Clinical Trials Group. *Br. J. Cancer* 73, 397–399
45. Martin, M.J. *et al.* (2013) Isolation and first total synthesis of PM050489 and PM060184, two new marine anticancer compounds. *J. Am. Chem. Soc.* 135, 10164–10171
46. Bai, R. *et al.* (1995) The spongistatins, potently cytotoxic inhibitors of tubulin polymerization, bind in a distinct region of the vinca domain. *Biochemistry* 34, 9714–9721
47. Tierno, M.B. *et al.* (2009) Microtubule binding and disruption and induction of premature senescence by disorazole C(1). *J. Pharmacol. Exp. Ther.* 328, 715–722
48. Prota, A.E. *et al.* (2014) A new tubulin-binding site and pharmacophore for microtubule-destabilizing anticancer drugs. *Proc. Natl. Acad. Sci. U. S. A.* 111, 13817–13821
49. Menchon, G. *et al.* (2018) A fluorescence anisotropy assay to discover and characterize ligands targeting the maytansine-site of tubulin. *Nat. Commun.* 29, 2106
50. Kobayashi, S. *et al.* (1994) Pironetin, a novel plant growth regulator produced by *Streptomyces* sp. NK10958. I. Taxonomy, production, isolation and preliminary characterization. *J. Antibiot.* 47, 697–702
51. Kobayashi, S. *et al.* (1994) Pironetin, a novel plant growth regulator produced by *Streptomyces* sp. NK10958. II. Structural elucidation. *J. Antibiot.* 47, 703–707
52. Kondoh, M. *et al.* (1998) Cell cycle arrest and antitumor activity of pironetin and its derivatives. *Cancer Lett.* 126, 29–32
53. Kondoh, M. *et al.* (1999) Apoptosis induction via microtubule disassembly by an antitumor compound, pironetin. *Biochem. J.* 340, 411–416
54. Watanabe, H. *et al.* (2000) Synthesis of pironetin and related analogs: studies on structure–activity relationships as tubulin assembly inhibitors. *J. Antibiot.* 53, 540–545
55. Usui, T. *et al.* (2004) The anticancer natural product pironetin selectively targets Lys352 of alpha-tubulin. *Chem. Biol.* 11, 799–806
56. Banuelos-Hernandez, A.E. *et al.* (2014) Studies of (–)-pironetin binding to alpha-tubulin: conformation, docking, and molecular dynamics. *J. Org. Chem.* 79, 3752–3764
57. Yang, J. *et al.* (2016) Pironetin reacts covalently with cysteine-316 of alpha-tubulin to destabilize microtubule. *Nat. Commun.* 7, 12103
58. Prota, A.E. *et al.* (2016) Pironetin binds covalently to alpha-Cys316 and perturbs a major loop and helix of alpha-tubulin to inhibit microtubule formation. *J. Mol. Biol.* 428, 2981–2988
59. Tanabe, K. (2017) Microtubule depolymerization by kinase inhibitors: unexpected findings of dual inhibitors. *Int. J. Mol. Sci.* 18, E2508
60. Maira, S.M. *et al.* (2012) Identification and characterization of NVP-BKM120, an orally available pan-class I PI3-kinase inhibitor. *Mol. Cancer Ther.* 11, 317–328
61. Massacesi, C. *et al.* (2013) Challenges in the clinical development of PI3K inhibitors. *Ann. N. Y. Acad. Sci.* 1280, 19–23
62. Brachmann, S.M. *et al.* (2012) Characterization of the mechanism of action of the pan class I PI3K inhibitor NVP-BKM120 across a broad range of concentrations. *Mol. Cancer Ther.* 11, 1747–1757
63. Bohnacker, T. *et al.* (2017) Deconvolution of Buparlisib's mechanism of action defines specific PI3K and tubulin inhibitors for therapeutic intervention. *Nat. Commun.* 8, 14683
64. Nawrotek, A. *et al.* (2011) The determinants that govern microtubule assembly from the atomic structure of GTP-tubulin. *J. Mol. Biol.* 412, 35–42
65. Pecoque, L. *et al.* (2012) A designed ankyrin repeat protein selected to bind to tubulin caps the microtubule plus end. *Proc. Natl. Acad. Sci. U. S. A.* 109, 12011–12016
66. Ayaz, P. *et al.* (2012) A TOG:alpha-tubulin complex structure reveals conformation-based mechanisms for a microtubule polymerase. *Science* 337, 857–860
67. Patel, D. *et al.* (2014) Advantages of crystallographic fragment screening: functional and mechanistic insights from a powerful platform for efficient drug discovery. *Prog. Biophys. Mol. Biol.* 116, 92–100
68. Janke, C. and Bulinski, J.C. (2011) Post-translational regulation of the microtubule cytoskeleton: mechanisms and functions. *Nat. Rev. Mol. Cell Biol.* 12, 773–786
69. Minoura, I. *et al.* (2013) Overexpression, purification, and functional analysis of recombinant human tubulin dimer. *FEBS Lett.* 587, 3450–3455
70. Ti, S.C. *et al.* (2016) Mutations in human tubulin proximal to the kinesin-binding site alter dynamic instability at microtubule plus- and minus-ends. *Dev. Cell* 37, 72–84
71. Borowiak, M. *et al.* (2015) Photoswitchable inhibitors of microtubule dynamics optically control mitosis and cell death. *Cell* 162, 403–411
72. Chen, S. *et al.* (2018) Near-infrared deep brain stimulation via upconversion nanoparticle-mediated optogenetics. *Science* 359, 679–684
73. Johansson, L.C. *et al.* (2017) A bright future for serial femtosecond crystallography with XFELs. *Trends Biochem. Sci.* 42, 749–762
74. Amos, L.A. (2011) What tubulin drugs tell us about microtubule structure and dynamics. *Semin. Cell Dev. Biol.* 22, 916–926
75. Howard, J. and Hyman, A.A. (2003) Dynamics and mechanics of the microtubule plus end. *Nature* 422, 753–758
76. Brouhard, G.J. and Rice, L.M. (2014) The contribution of alpha-beta-tubulin curvature to microtubule dynamics. *J. Cell Biol.* 207, 323–334
77. Akhmanova, A. and Steinmetz, M.O. (2008) Tracking the ends: a dynamic protein network controls the fate of microtubule tips. *Nat. Rev. Mol. Cell Biol.* 9, 309–322
78. Trigili, C. *et al.* (2016) Structural determinants of the dictyostatin chemotype for tubulin binding affinity and antitumor activity against taxane- and epothilone-resistant cancer cells. *ACS Omega* 1, 1192–1204
79. Nettles, J.H. *et al.* (2004) The binding mode of epothilone A on alpha,beta-tubulin by electron crystallography. *Science* 305, 866–869

80. Howes, S.C. *et al.* (2017) Structural differences between yeast and mammalian microtubules revealed by cryo-EM. *J. Cell Biol.* 216, 2669–2677
81. Zhou, P. *et al.* (2016) Potent antitumor activities and structure basis of the chiral beta-lactam bridged analogue of combretastatin A-4 binding to tubulin. *J. Med. Chem.* 59, 10329–10334
82. Niu, L. *et al.* (2017) Structure of 4'-demethylepipodophyllotoxin in complex with tubulin provides a rationale for drug design. *Biochem. Biophys. Res. Commun.* 493, 718–722
83. Dohle, W. *et al.* (2018) Quinazolinone-based anticancer agents: synthesis, antiproliferative SAR, antitubulin activity, and tubulin co-crystal structure. *J. Med. Chem.* 61, 1031–1044
84. Fu, Z. *et al.* (2018) Design, synthesis and biological evaluation of anti-pancreatic cancer activity of plinabulin derivatives based on the co-crystal structure. *Bioorg. Med. Chem.* 26, 2061–2072
85. Protá, A.E. *et al.* (2014) The novel microtubule-destabilizing drug BAL27862 binds to the colchicine site of tubulin with distinct effects on microtubule organization. *J. Mol. Biol.* 426, 1848–1860
86. Ahmad, S. *et al.* (2016) Destabilizing an interacting motif strengthens the association of a designed ankyrin repeat protein with tubulin. *Sci. Rep.* 6, 28922
87. Weinert, T. *et al.* (2017) Serial millisecond crystallography for routine room-temperature structure determination at synchrotrons. *Nat. Commun.* 8, 542
88. Gaspari, R. *et al.* (2017) Structural basis of cis- and trans-combretastatin binding to tubulin. *Chem* 2, 102–113
89. McNamara, D.E. *et al.* (2015) Structures of potent anticancer compounds bound to tubulin. *Protein Sci.* 24, 1164–1172
90. Zhou, P. *et al.* (2018) Design, synthesis, biological evaluation and cocrystal structures with tubulin of chiral beta-lactam bridged combretastatin A-4 analogues as potent antitumor agents. *Eur. J. Med. Chem.* 144, 817–842
91. Armst, K.E. *et al.* (2018) A potent, metabolically stable tubulin inhibitor targets the colchicine binding site and overcomes taxane resistance. *Cancer Res.* 78, 265–277
92. Wang, Y. *et al.* (2016) Structures of a diverse set of colchicine binding site inhibitors in complex with tubulin provide a rationale for drug discovery. *FEBS J.* 283, 102–111
93. Barbier, P. *et al.* (2010) Stathmin and interfacial microtubule inhibitors recognize a naturally curved conformation of tubulin dimers. *J. Biol. Chem.* 285, 31672–31681
94. Jost, M. *et al.* (2017) Combined CRISPRi/a-based chemical genetic screens reveal that rigosertib is a microtubule-destabilizing agent. *Mol. Cell* 68, 210–223
95. Marangon, J. *et al.* (2016) Tools for the rational design of bivalent microtubule-targeting drugs. *Biochem. Biophys. Res. Commun.* 479, 48–53
96. Cheng, J. *et al.* (2018) Structure of a benzylidene derivative of 9 (10H)-anthracenone in complex with tubulin provides a rationale for drug design. *Biochem. Biophys. Res. Commun.* 495, 185–188
97. Bueno, O. *et al.* (2018) High-affinity ligands of the colchicine domain in tubulin based on a structure-guided design. *Sci. Rep.* 8, 4242
98. Canela, M.D. *et al.* (2017) Antivascular and antitumor properties of the tubulin-binding chalcone TUB091. *Oncotarget* 8, 14325–14342
99. Leverett, C.A. *et al.* (2016) Design, synthesis, and cytotoxic evaluation of novel tubulysin analogues as ADC payloads. *ACS Med. Chem. Lett.* 7, 999–1004
100. Saez-Calvo, G. *et al.* (2017) Triazolopyrimidines are microtubule-stabilizing agents that bind the vinca inhibitor site of tubulin. *Cell Chem. Biol.* 24, 737–750